

STEEL COLUMNS UNDER MULTI-AXIS CYCLIC LOADING: EXPERIMENTS, MODELS AND DESIGN RECOMMENDATIONS

Dimitrios G. Lignos

Associate Professor

Ecole Polytechnique Fédérale de Lausanne (EPFL)

Lausanne, Switzerland

E-mail: dimitrios.lignos@epfl.ch

Ahmed Elkady

Post-Doctoral Research Scientist

Ecole Polytechnique Fédérale de Lausanne (EPFL)

Lausanne, Switzerland

E-mail: ahmed.elkady@epfl.ch

Yusuke Suzuki

Senior Researcher

Nippon Steel and Sumitomo Metal Corporation

Tokyo, Japan

E-mail: suzuki.s2k.yusuke@jp.nssmc.com

1. ABSTRACT

This paper summarizes the findings of a long term experimental program corroborated with detailed finite element simulations that investigated the hysteretic behavior of wide-flange columns of steel moment-resisting frames (MRFs) designed in highly seismic regions. Several aspects of the steel column behavior are thoroughly investigated. It is shown that steel column axial shortening is a failure mode that strongly influences the steel column stability under earthquake-induced loading. The amount of axial shortening can be considerably different in interior columns compared to end (exterior) columns that experience transient axial load demands due to dynamic overturning effects. Axial shortening is typically followed by column out-of-plane deformations that become maximum near the dissipative plastic hinge zone and migrate near the column top end. This failure mode is strongly influenced by the considered boundary conditions. Routinely used symmetric loading histories provide insufficient information for modeling the cyclic deterioration in flexural strength and stiffness of steel columns near collapse. Design recommendations to improve the steel column stability under cyclic loading are discussed.

2. INTRODUCTION

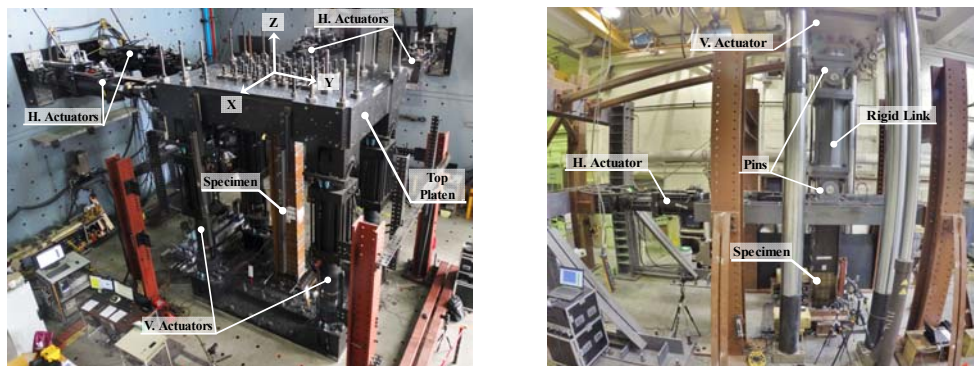
With the advent of performance-based earthquake engineering, nonlinear modeling of structural components is essential in order to assess the seismic performance of frame buildings from the onset of damage through the occurrence of structural collapse. Historically, the ASCE 41 [1] nonlinear modeling provisions have been employed for this purpose. Limited experimental evidence primarily from small scale wide-shape steel columns [2,3] suggests that these members may behave much better than expected in reality. However, steel MRF columns are subjected to complex cyclic loading. This is due

to the randomness of the imposed earthquake loading history, the dynamic overturning effects that impose transient axial load demands to end columns compared to interior columns within the same story, as well as the bidirectional loading due to the 3-dimensional ground motion shaking. Other issues associated with the effect of member end boundary conditions have also been overlooked because in most cases steel columns were tested with simplified boundary conditions. In particular, these were either fixed-fixed or fixed-free (i.e., cantilever fashion). More recently, the earthquake-induced collapse risk quantification of frame buildings has gained increased attention [4,5]. In this context, a number of researchers [6,7] have highlighted the lack of monotonic tests that push structural components far into the inelastic range in order to properly quantify their ultimate deformation capacity.

In order to satisfy all the aforementioned objectives, a 6-year experimental program has been conducted that examined the hysteretic behavior of steel columns subjected to multi-axis cyclic loading. This program is corroborated by detailed finite element simulations that facilitated the expansion of the test results to a wide range of steel column sizes currently used in the seismic design practice. This paper summarizes the main findings of this program as well a discussion on current efforts to refine the current seismic design provisions associated with the steel column stability.

3. TEST MATRIX AND EXPERIMENTAL SETUP

The test matrix including the geometric and loading parameters of the test specimens is summarized in *Table 1*. It consists of five sets of cross-section sizes including deep cross-sections (W16 and W24) as well as shallow sections (i.e., W14). Each set includes a number of nominally identical steel columns fabricated by ASTM A992 Grade 50 steel (i.e., nominal yield stress, $f_y = 345\text{MPa}$). The test specimens are selected by considering (a) the local slenderness ratios of highly compact cross-sections as per AISC 341-10 [8]; and (b) commonly used cross-sections in typical mid-rise steel frame buildings with MRFs [9]. The specimens are tested in two separate testing facilities that are shown in *Fig. 1*. At Ecole Polytechnique Montréal (EPM), members are tested in full length (i.e., approximately 4.5m) in a 6-degree-of-freedom-system (see *Fig. 1a*) such that the effects of (a) member slenderness; (b) boundary effects; and (c) the bidirectional loading on the column performance can be assessed. At the Jamieson Structures Laboratory (McGill University) steel columns are tested in a cantilever fashion (i.e., inflection point is assumed to be constant). In this case, emphasis is placed on the influence of local slenderness, the transient axial load and the influence of loading history on the steel column hysteretic performance.



(a) 6-DOF test setup at EPM (b) multi-axis column test simulator at McGill

Fig. 1 Experimental setup for steel column testing

Specimen ID	Cross-	Lateral loading protocol	Axial loading
A-C1	W24x146	AISC-symmetric (fixed-fixed)	$P_g/P_{ye} = 0.2$
A-C2		AISC-symmetric (fixed-fixed)	$P_g/P_{ye} = 0.5$
A-C3		AISC-symmetric (fixed-flexible)	$P_g/P_{ye} = 0.2$
A-C4		Collapse-consistent (fixed-flexible)	$P_g/P_{ye} = 0.2$
A-C5		Bidir.-symmetric (fixed-flexible)	$P_g/P_{ye} = 0.2$
A-C6		Bidir.-Collapse-consistent (fixed-flexible)	$P_g/P_{ye} = 0.2$
A-C7	W24x84	AISC-symmetric (fixed-flexible)	$P_g/P_{ye} = 0.2$
A-C8		Collapse-consistent (fixed-flexible)	$P_g/P_{ye} = 0.2$
A-C9		Bidir.-symmetric (fixed-flexible)	$P_g/P_{ye} = 0.2$
A-C10		Bidir.-Collapse-consistent (fixed-flexible)	$P_g/P_{ye} = 0.2$
B-C11	W14X53	Monotonic	$P_g/P_{ye} = 0.3$
B-C12		AISC-symmetric	$P_g/P_{ye} = 0.3$
B-C13		Collapse-consistent #1	$P_g/P_{ye} = 0.3$
B-C14		Collapse-consistent #1	Varying
B-C15		Collapse-consistent #2	$P_g/P_{ye} = 0.3$
B-C16		Collapse-consistent #2	Varying
C-C17	W14x61	Monotonic	$P_g/P_{ye} = 0.3$
C-C18		Monotonic	$P_g/P_{ye} = 0.5$
C-C19		Collapse-consistent	$P_g/P_{ye} = 0.5$
C-C20		AISC-symmetric	Varying
C-C21		AISC-symmetric	$P_g/P_{ye} = 0.3$
C-C22		Collapse-consistent #1	$P_g/P_{ye} = 0.3$
C-C23		Collapse-consistent #1	Varying
D-C24	W14x82	Monotonic	$P_g/P_{ye} = 0.3$
D-C25		Monotonic	$P_g/P_{ye} = 0.5$
D-C26		AISC-symmetric	$P_g/P_{ye} = 0.5$
D-C27		AISC-symmetric	$P_g/P_{ye} = 0.75$
D-C28		AISC-symmetric	$P_g/P_{ye} = 0.3$
D-C29		Collapse-consistent #1	$P_g/P_{ye} = 0.3$
D-C30		Collapse-consistent #1	Varying
E-C31	W16x89	Monotonic	$P_g/P_{ye} = 0.3$
E-C32		Monotonic	$P_g/P_{ye} = 0.5$
E-C33		AISC-Symmetric	$P_g/P_{ye} = 0.5$
E-C34		AISC-Symmetric	Varying

Table 1. Summary of test matrix for experimental testing of wide flange steel columns

In brief, nominally identical specimens from different sets are subjected to a range of constant compressive axial load ratios, $P_g/P_{ye} = 0.3$ and 0.5 (in which, P_g is the gravity load that is applied to the column and P_{ye} is the expected axial yield strength of the respective steel cross-section) coupled with monotonic and/or cyclic lateral loading. In order to investigate the effect of the lateral loading history on the steel column behavior, several specimens are subjected to a collapse-consistent loading protocol that represents the ratcheting behavior of a column in a steel MRF that approaches collapse [10]. In order to investigate the effect of high axial load demands on the steel column plastic deformation, the W14x82, W16x89 and W24x146 test specimens are subjected to excessive axial compressive ratios $P_g/P_{ye} = 0.5$ (i.e., $P_g/P_{cr} > 0.5$; in which P_{cr} is the critical load of a column). Finally, in order to further investigate the differences of the hysteretic response

between interior and end columns, several specimens are subjected to varying axial load synchronized with the AISC symmetric and a collapse-consistent lateral loading protocol [10]. The employed lateral loading histories are summarized in *Fig. 2*. They are categorized as unidirectional (see *Figs. 2a* and *b*) and bidirectional (see *Figs. 3c* and *d*). Referring to *Table 1*, a steel column can be subjected to high axial compressive loads (i.e., $0.75P_{ye}$) as well as relatively high axial tensile loads (i.e., $-0.20P_{ye}$) after the gravity offset is applied. Finally, in order to assess the boundary condition effects on the steel column hysteretic behavior, nominally identical specimens (i.e., W24x146 and W24x84) are considered with both a fixed and a flexible top end boundary.

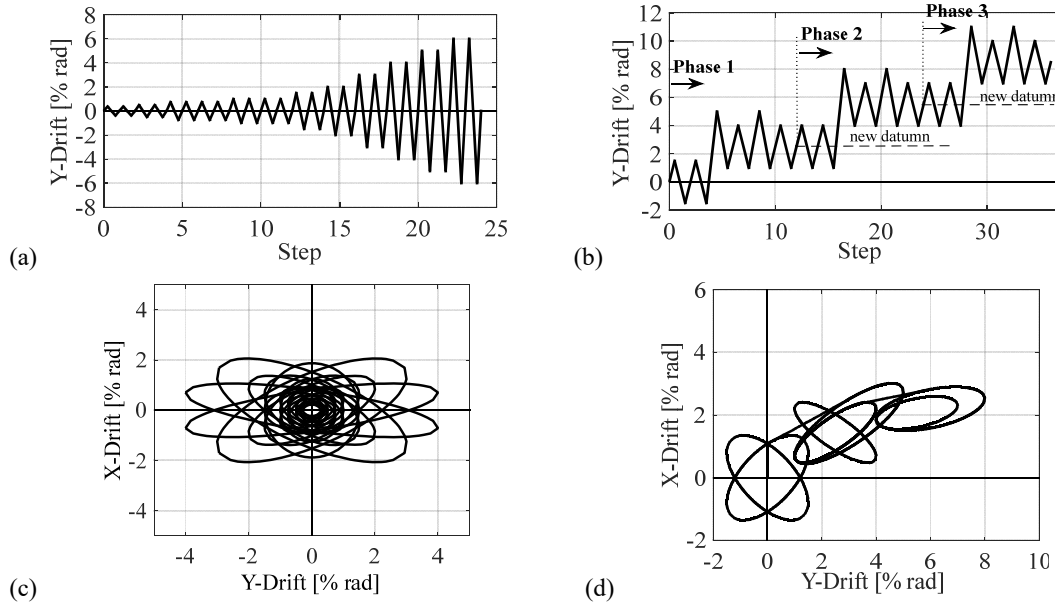


Fig. 2 Lateral loading protocols utilized in the testing program

4. TEST RESULTS AND DISCUSSION

This section discusses a number of findings from the experimental program outlined in Section 3. Emphasis is placed on the effect of boundary conditions, the bidirectional lateral loading, the transient axial load demands and the lateral loading history on the overall steel column stability under cyclic loading. Several other findings can be found in great detail in prior publications by the authors [11,15].

4.1 Effect of boundary conditions on column behavior

Referring to *Table 1*, Series-A tests examined the effect of member end boundary conditions on the column cyclic behavior. This effect is examined by comparing the performance of the two column specimens, A-C1 and A-C3. Specimen A-C1 was tested with a rotationally-fixed top while specimen A-C3 had a rotationally-flexible top. The latter is a realistic representation of the flexible rotational stiffness of beam-to-column connections intersecting first story steel MRF columns at their top end. *Figure 3a* shows that both specimens exhibited very similar moment-rotation behavior at their base; yet, the onset of local buckling occurred a bit later in specimen A-C3, due to its larger flexibility. Referring to *Fig. 3b*, the difference in behavior at the column top between the two specimens is appreciable. While specimen A-C1 experienced larger amount of plastic deformation and strength deterioration at its top end (similar to the column base), specimen A-C3 experienced limited amount of plastic deformation ($\approx 1.5\%$) as it yielded much later

during the imposed loading history. The latter case is representative of capacity-designed first-story MRF columns that are expected to yield only at their base.

At drifts less than 3%, specimen A-C1 experienced larger out-of-plane deformations near the plastified dissipative zones at the member ends as well as larger twisting angles along its height compared to specimen A-C3. This is attributed to the simultaneous loss of flexural and torsional stiffness at both column ends in specimen A-C1 at relatively smaller drifts [15]. At drifts larger than 3%, the out-of-plane deformations, concentrated only at the base of specimen A-C3, increased rapidly due to the increasing weak-axis member P-Delta demands. This is shown in *Fig. 3c*. In particular, the out-of-plane deformations and twisting angles of specimen A-C3 became almost double of those measured in specimen A-C1. These deformations are expected to be amplified in slender columns (i.e., member slenderness ratios, L_b/r_y larger than $L_b/r_y > 80$). In summary, this highlights that the expected column failure mode, and its associated performance can be misleading if fixed-end boundary conditions are considered.

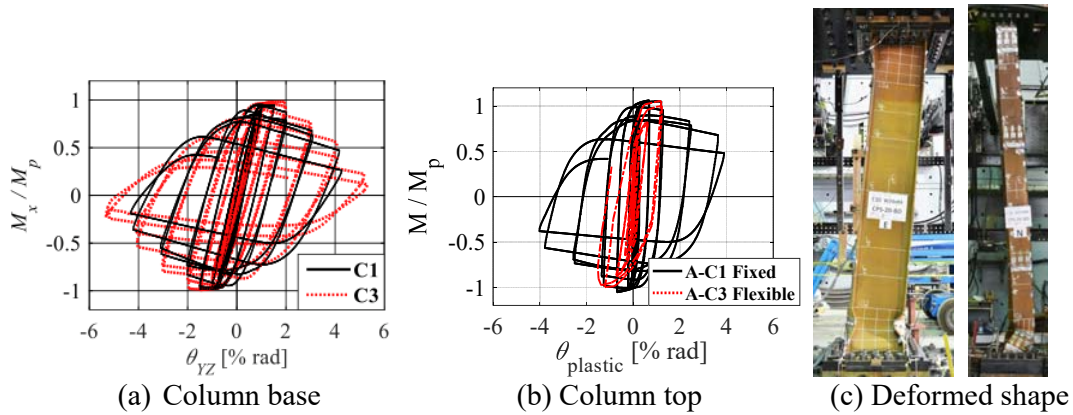


Fig. 3 Effect of column end boundary conditions on the steel column performance

4.2 Bidirectional versus unidirectional behavior

Pair specimens A-C8 - A-C10 and A-C7 – A-C9 utilized the same cross-sections, boundary conditions, and applied axial compressive load (see *Table 1*). The hysteretic behavior of the two specimens is compared in terms of their deduced moment-rotation relation in *Fig. 4*. From the same figure, the plastic deformation capacity of a column is practically not sensitive to the bidirectional lateral loading. This observation holds true for the range of sections that were tested regardless of the type of lateral loading (i.e., symmetric or collapse-consistent). Nonetheless, for story drift-ratios larger than 3% radians, the rate of cyclic deterioration in flexural strength of a column is slightly larger under bidirectional lateral loading compared to that from unidirectional lateral loading. This is attributed to the additional flexural demands in the weak-axis direction of the beam-column cross section. This effect is practically negligible on the first-cycle envelope curves of nominally identical specimens. In that respect, if the objective is to construct a first-cycle envelope curve for a steel column for the nonlinear evaluation of steel MRFs under seismic loading this can be done with experimental data based on unidirectional loading protocols.

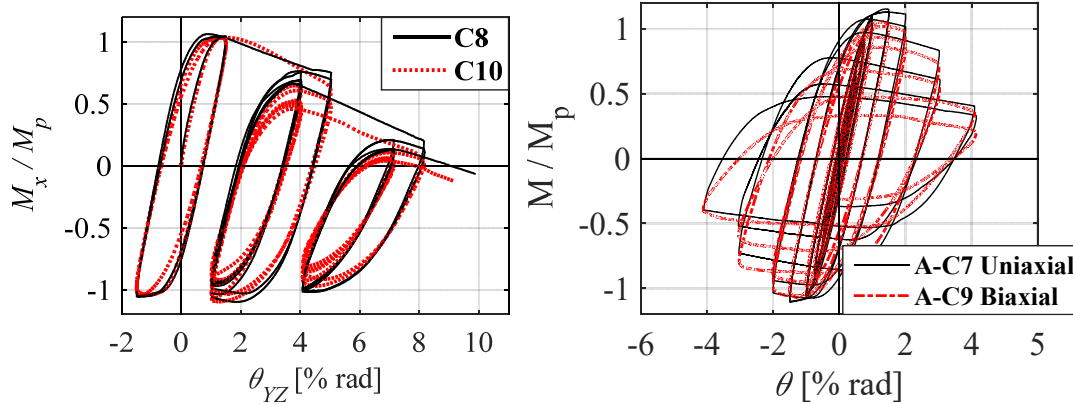


Fig. 4 Effect of bidirectional versus unidirectional lateral loading histories on steel column performance

4.3 Effect of transient axial load demands

During an earthquake, a typical first-story interior column experiences small fluctuations in axial load demands due to overturning moments. Hence, these columns are more-or-less subjected to a constant compressive gravity axial load. The gravity load is about 20% P_{ye} in modern steel MRF buildings [10] while it can reach 50% P_{ye} in existing steel MRF buildings [16]. End columns, can experience large fluctuations in axial load demands ranging from 75% in compression and 20% in tension [10]. In that respect, the effect of varying, versus constant, axial load demands on the column behavior is assessed. *Figure 5* compares the moment-rotation and axial shortening history of two nominally identical specimens, E-C33 and E-C34, subjected to two types of axial load demands. Referring to *Fig. 5*, the asymmetric cyclic behavior of specimen E-C33 under varying axial load (i.e., end columns) is noticeable. This specimen buckled earlier and sustained high in-cycle strength deterioration, as inferred by the steep post-buckling slope in the positive loading direction (i.e., with increasing compressive axial load). In the negative direction, no in-cycle deterioration is observed due to the straightening of flange buckling while the axial load decreases.

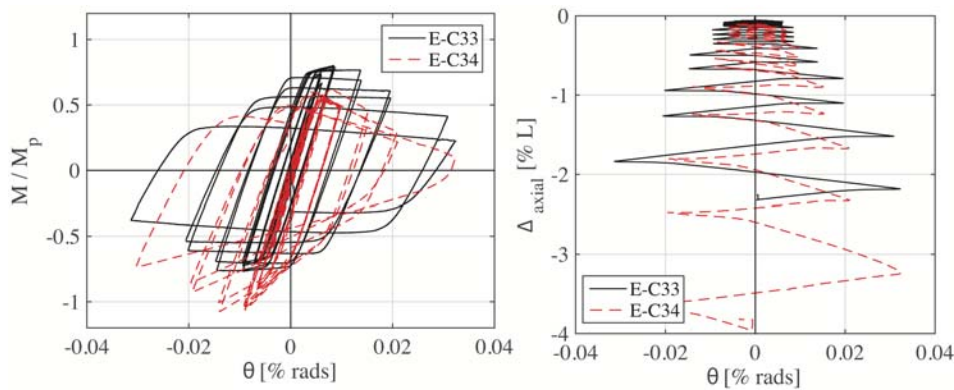


Fig. 5 Effect of axial load demands on steel column stability

Referring to *Fig. 5b*, the level of axial shortening experienced by end and interior first-story columns can be significantly different. This is discussed in more detail in the subsequent section.

4.4 Effect of lateral loading history

Figure 6a compares the deduced moment versus chord rotation of the W14x53 specimens, respectively, under various lateral loading protocols (i.e., Specimens B-C11 to B-C14). From this figure, the flexural strength deterioration of this column became zero at chord rotations larger than 15% based on the monotonic backbone curve. In addition, the flexural strength of a test specimen deteriorated in the positive and negative loading direction when the axial load was kept constant. This is due to the formation of local buckling in both flanges of a steel column. Note that when varying axial load is coupled with lateral drift demands then the flexural strength of a steel column does not typically deteriorate in the negative loading direction. This is due to the position of the cross-sectional neutral axis. Therefore, it is expected that interior steel columns would typically lose faster their flexural strength and axial load carrying capacity compared to end columns within the same MRF story.

Referring to Fig. 6a, when a symmetric cyclic lateral loading protocol is employed the steel column flexural strength deteriorates a lot faster than a nominally identical specimen that experiences a collapse-consistent loading protocol. This is due to the large number of inelastic loading cycles included in a symmetric cyclic lateral loading protocol. However, columns in steel MRFs subjected to ordinary or near-fault ground motions would typically experience few inelastic cycles followed by a large monotonic push prior to structural collapse [7]. Prior studies associated with the collapse assessment of frame buildings have highlighted that the pre- and post-capping plastic rotation capacities are fundamental quantities for the reliable collapse assessment [5,7]. Referring to Fig. 6a, this information becomes available only when a combination of a monotonic and a collapse-consistent lateral loading protocol is employed for experimental testing of steel columns. Same findings hold true for the rest of the tested specimens.

Figure 6b illustrates the steel column axial shortening versus chord rotation relations for the same specimens discussed previously. The axial shortening is normalized with respect to the column height. Referring to Fig. 6b, when a constant compressive axial load is applied on a steel column its axial shortening accumulates in both the positive and negative loading directions regardless of the cross-section shape. The amount of axial shortening depends on the number of inelastic loading cycles of the respective lateral loading protocol as well as the applied axial load. End columns would experience 6 to 7 times smaller axial shortening compared to interior columns. The reason is that an end column experiences tensile load in the negative loading direction due to dynamic overturning effects. In order to limit the amount of column axial shortening an obvious solution can be the reduction of the local slenderness limits for highly ductile members [17].

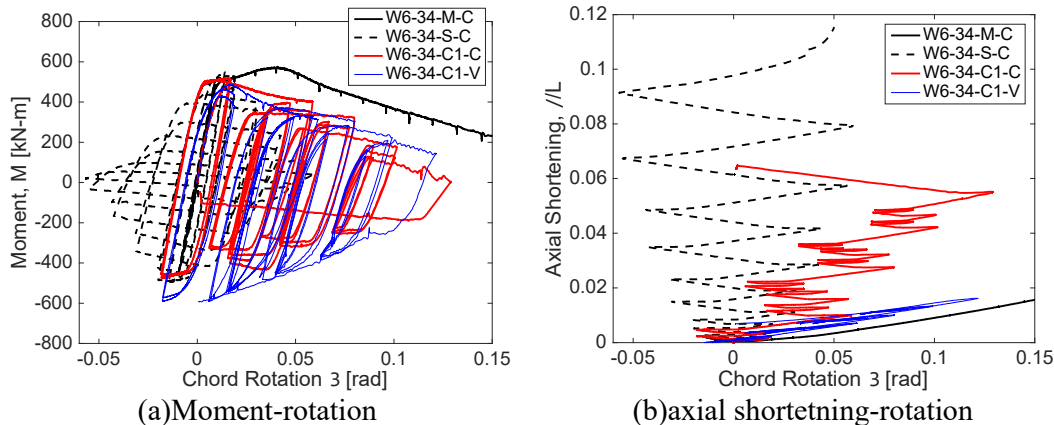
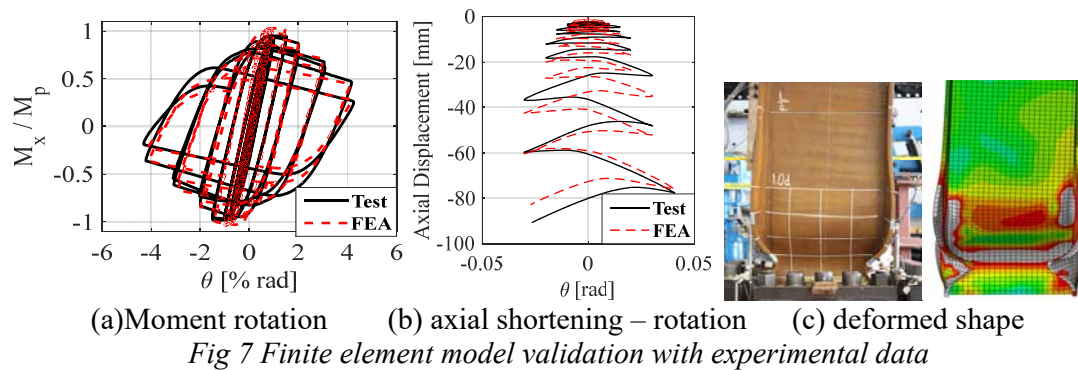


Fig. 6 Effect of lateral loading history on steel column stability

5. FINITE ELEMENT MODELING

In parallel with the experimental program outlined in the previous sections, an extensive finite element (FE) parametric study was conducted to investigate several aspects related to the hysteretic behavior of steel wide-flange columns. To this end, a detailed finite element modeling approach was utilized. The modeling approach considers material nonlinearity and residual stresses commonly found in hot-rolled sections. The FE modeling approach was validated with the experimental data from the full-scale testing program discussed earlier. A sample comparison of the deduced moment-rotation and axial displacement-rotation relations and the ones predicted by FE analysis is shown in *Figs. 7a* and *7b*, respectively. A sample comparison of the local deformation profiles between tests and FE models are shown in *Fig. 7c*. More details can be found in [17]. Overall, the FE modeling approach is able to capture with reasonable accuracy the nonlinear behavior as well as local and global instabilities of steel columns regardless of the employed cross-section, geometry, boundary conditions and the applied loading protocol. To assess the behavior of a bigger pool of cross-sections used in practice more than 40 cross-sections ranging from W12 to W36 are examined. Emphasis is placed on stocky (set W1), moderately stocky (set W2), slender but highly ductile (set W3) and moderately compact (set W4) cross sections.



5.1 Column axial shortening and proposed design recommendations

The experimental results as well as the finite element studies reveal that the column axial shortening is an important failure mode, particularly in columns under relatively large compressive axial loads. This issue becomes more critical in high-rise steel frame buildings, where differential axial shortening levels between interior and end columns can lead to global structural instability. To illustrate that, *Fig 8* shows the progression of axial shortening (Δ_{axial}) normalized with respect to the column undeformed length L , versus the cumulative inelastic rotation for $P_g/P_{ye}=20\%$ (see *Fig. 8a*) and $P_g/P_{ye}=50\%$ (see *Fig. 8b*). This figure shows that at a 2% drift amplitude, all columns with $P_g/P_{ye}=20\%$ and highly ductile cross-sections (i.e., Set W1, W2, and W3) shorten by less than 0.7% L . For axial load levels, larger than 20% P_{ye} , column axial shortening exceeds 1% L when the least compact cross-sections (i.e., Set W3) are utilized. Note that, even at axial load ratios less than 20% P_{ye} , an axial shortening ratio larger than 1% L is also developed in all columns at 4% drift amplitude. Based on test findings discussed in the previous sections, it was shown that when axial shortening exceeds 1% L , global instabilities start to develop rapidly. To this end, to achieve an axial shortening level less than 1% L at drift levels associated with design-basis seismic events (i.e., 2% rads), the current compactness limits according to the AISC-341-10 [8] provisions need to be reduced by two-thirds and the axial load demands need to be limited to 30% P_{ye} .

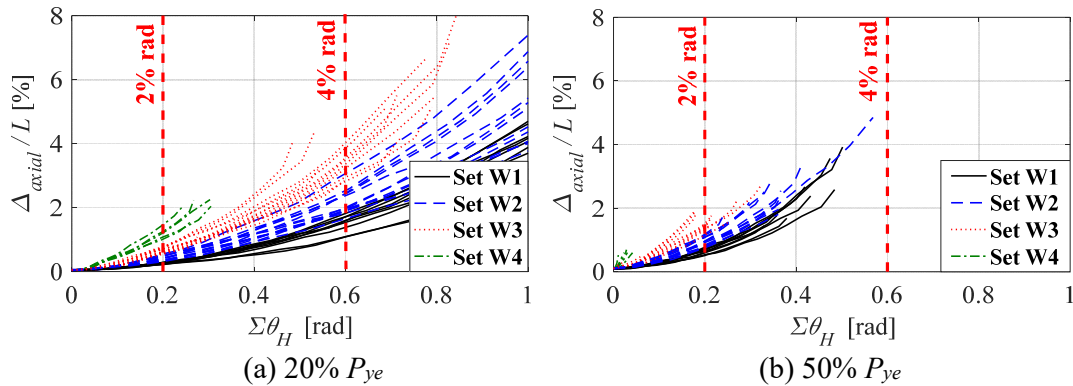


Fig 8 Normalized column axial shortening versus cumulative inelastic rotation subjected to symmetric loading protocol

6. CONCLUSIONS

This paper discusses the findings of an extensive testing program corroborated by detailed finite element analysis studies on wide flange steel columns subjected to multi-axis cyclic loading similar to that seen in first story steel columns of steel moment-resisting frames (MRFs). The selected shapes represent the current common design practice in North America. Several parameters that affect the hysteretic behavior of steel columns were interrogated. The main findings are summarized as follows:

- After the onset of local buckling, the column axial shortening increases exponentially with respect to the cumulative inelastic rotation. At $P_g/P_{ye}=20\%$ and $\theta=4\%$ rads, columns that utilized cross-sections near λ_{hd} limits (i.e., set W3) as per [8] ($32.5 \leq h/t_w \leq 43$ and $5.5 \leq b_f/2t_f \leq 7$) shorten by about $6\% L$.
- Steel columns subjected to bidirectional lateral loading develop the center of the local buckling wave further away from the column base compared to those subjected to unidirectional lateral loading. These effects are more pronounced for column members in which the member slenderness is $L_b/r_y > 80$. However, if the objective is to develop simplified backbone component models for nonlinear modeling of steel columns to conduct nonlinear static analysis of steel MRFs, no adjustments are necessary to the plastic deformation capacity of steel columns due to bidirectional lateral loading.
- The plastic deformation of steel columns subjected to a collapse-consistent loading protocol is at least twice larger than those subjected to a symmetric cyclic loading protocol. Notably, at large drifts (i.e., larger than 4%), steel columns subjected to a collapse-consistent loading protocol shortened 5 times less than those subjected to a symmetric loading protocol. These findings underscore the importance of utilizing realistic loading histories for characterizing the “ratcheting” hysteretic behavior of structural components from the onset of damage through structural collapse.
- The flexural strength of a steel column under varying axial load deteriorates more rapidly than that of the same column under constant compressive axial load due to the high axial compressive load at fairly small lateral deformation amplitudes. However, at large lateral deformations, the effect of cumulative damage on the buckled flange of steel columns under varying axial load is typically smaller than that of identical steel columns subjected to a constant compressive axial load ratio. This difference implies that interior steel columns would typically lose faster their flexural strength compared to end columns within the same story of a steel MRF.

- A reduction to about two-thirds of the current compactness limit for highly ductile wide-flange cross-sections as per [8] used in first story steel columns in steel MRFs.
 - An upper limit of 30% P_{ye} for the axial load in columns as part of steel special MRFs.
- In all cases, the effect of column base flexibility due to the interaction of the steel column with the reinforced concrete footing was neglected. This issue deserves more attention in future studies.

7. ACKNOWLEDGMENTS

This study was based on work supported by the National Science and Engineering Research Council of Canada (NSERC) under the Discovery Grant Program. Funding was also provided by the Canadian Institute of Steel Construction (CISC) and the Swiss National Science Foundation (Award No. 200021_169248). This financial support is gratefully acknowledged. Any opinions, findings, and conclusions or recommendations expressed in this paper are those of the authors and do not necessarily reflect the views of sponsors.

8. REFERENCES

- [1] ASCE “Seismic evaluation and retrofit of existing buildings”, *ASCE/SEI-41-13*, 2014.
- [2] MacRae GA “The seismic response of steel frames”, *PhD Dissertation*, Christchurch, New Zealand, Department of Civil Engineering, University of Canterbury, 1990.
- [3] Popov E, Bertero V.V., and Chantramouli S. “Hysteretic behavior of steel columns”, *Report UCB/EERC-75-11*, Earthquake Engineering Research Center (EERC), University of California, Berkeley, 1975.
- [4] FEMA “Quantification of building seismic performance factors”, *Report FEMA-P695*, 2009.
- [5] Zareian F, Krawinkler H, Ibarra L, and Lignos DG “Basic concepts and performance measures in prediction of collapse of buildings under earthquake ground motions”, *The Structural Design of Tall and Special Buildings*, Vol. 19, No. 1-2, 2014, pp. 167-181.
- [6] Krawinkler H, “Loading histories for cyclic tests in support of performance assessment of structural components”, Pacific Earthquake Engineering Research Center Annual Conference. San Francisco, California, 2009.
- [7] Lignos DG, Krawinkler H, and Whittaker AS “Prediction and validation of sidesway collapse of two scale models of a 4-story steel moment frame”, *Earthquake Engineering & Structural Dynamics*, Vol. 40, No. 7, 2011, pp. 807-825.
- [8] AISC “Seismic provisions for structural steel buildings”, ANSI/AISC 341-10, Chicago, IL: American Institute for Steel Construction, 2010.
- [9] Elkady A, and Lignos DG “Effect of gravity framing on the overstrength and collapse capacity of steel frame buildings with perimeter special moment frames”, *Earthquake Engineering & Structural Dynamics*, Vol. 44, No. 8, 2015, pp. 1289-1307.
- [10] Suzuki Y, and Lignos DG “Development of loading protocols for experimental testing of steel columns subjected to combined high axial load and lateral drift demands near collapse”, 10th National Conference on Earthquake Engineering,

Anchorage, Alaska: EERI; 2014.

- [11] Elkady A, and Lignos DG “Dynamic stability of deep slender wide-flange steel columns-full scale experiments”, SSRC Annual Stability Conference, Structural Stability Research Council, Orlando, Florida: Structural Stability Research Council, 2016.
- [12] Lignos DG, Cravero J, and Elkady A “Experimental investigation of the hysteretic behavior of wide-flange steel columns under high axial load and lateral drift demands”, 11th Pacific Structural Steel Conference, Shanghai, China, 2016.
- [13] Elkady A, and Lignos DG “Stability requirements of deep steel wide-flange columns under cyclic loading”, SSRC Annual Stability Conference, Structural Stability Research Council, San Antonio, Texas: Structural Stability Research Council, 2017.
- [14] Suzuki Y, and Lignos DG “Large scale collapse experiments of wide flange steel beam-columns”, 8th International Conference on Behavior of Steel Structures in Seismic Areas (STESSA), Shanghai, China, 2015.
- [15] Elkady A, and Lignos DG “Full-scale testing of wide-flange steel columns under multi-axis cyclic loading: Loading sequence, boundary effects and out-of-plane brace force demands”, *ASCE Journal of Structural Engineering*, 2017 (in press).
- [16] Bech D, Tremayne B, and Houston J “Proposed changes to steel column evaluation criteria for existing buildings”, 2nd ATC-SEI Conference on Improving the Seismic Performance of Existing Buildings and Other Structures, San Francisco, CA, USA, 2015.
- [17] Elkady A, and Lignos DG “Analytical investigation of the cyclic behavior and plastic hinge formation in deep wide-flange steel beam-columns”, *Bulleting of Earthquake Engineering*, Vol. 13, No. 4, 2015, pp. 1097-1118.

**Μεταλλικά υποστυλώματα υπό ανακυκλιζόμενη φόρτιση: Πειράματα,
προσομοιώματα και κανονιστικές διατάξεις**

Dimitrios G. Lignos

Associate Professor

Ecole Polytechnique Fédérale de Lausanne (EPFL)

Lausanne, Switzerland

E-mail: dimitrios.lignos@epfl.ch

Ahmed Elkady

Post-Doctoral Research Scientist

Ecole Polytechnique Fédérale de Lausanne (EPFL)

Lausanne, Switzerland

E-mail: ahmed.elkady@epfl.ch

Yusuke Suzuki

Senior Researcher

Nippon Steel and Sumitomo Metal Corporation

Tokyo, Japan

E-mail: suzuki.s2k.yusuke@jp.nssmc.com

ΠΕΡΙΛΗΨΗ

Το άρθρο παρουσιάζει τα συμπεράσματα από μια σειρά πειραματικών και αριθμητικών μελετών για τον χαρακτηρισμό της συμπεριφοράς μεταλλικών υποστυλωμάτων πλαισίων υπό ανακυκλιζόμενη φόρτιση. Η «αξονική σύνθλιψη» (κόντεμα) του μέλους λόγω τοπικού λυγισμού είναι άμεσα συσχετισμένος με την ευστάθειά του υπό ανακυκλιζόμενη φόρτιση. Η «αξονική σύνθλιψη» εσωτερικών υποστυλωμάτων υπό σταθερό θλιπτικό αξονικό φορτίο είναι πολύ μεγαλύτερη σε σχέση με την αντίστοιχη σύνθλιψη εξωτερικών υποστυλωμάτων που υπόκεινται σε μεταβαλλόμενα αξονικά φορτία λόγω της δυναμικής φόρτισης. Η ευστάθεια ενός μεταλλικού υποστυλώματος υπό ανακυκλιζόμενη φόρτιση χαρακτηρίζεται από μεγάλες μετατοπίσεις εκτός επιπέδου της εγκάρσιας φόρτισης οι οποίες μεγιστοποιούνται κοντά στη ζώνη πλαστικοποίησης του υποστυλώματος λόγω διαρροής και τοπικού λυγισμού. Η συγκεκριμένη μορφή γεωμετρικής αστάθειας επηρεάζεται από τις συνοριακές συνθήκες του αντίστοιχου υποστυλώματος. Συμμετρικά πρωτόκολλα φόρτισης τα οποία έχουν χρησιμοποιηθεί κατά κόρον σε διάφορες πειραματικές μελέτες στο παρελθόν δεν παρέχουν αντιπροσωπευτικά στοιχεία για τη συμπεριφορά και τον τρόπο αστοχίας ενός υποστυλώματος σε μεγάλες μετατοπίσεις που σχετίζονται με τη κατάρρευση μεταλλικών κατασκευών σε μεγάλους σεισμούς. Το άρθρο περιλαμβάνει μια σειρά προτάσεων για τη βελτίωση των κανονιστικών διατάξεων που

αφορούν τον σεισμικό σχεδιασμό μεταλλικών υποστυλωμάτων υπό ανακυκλιζόμενη φόρτιση.